Wood–Polymer Composites Prepared by the *In Situ* Polymerization of Monomers Within Wood

Yong-Feng Li,[1] Yi-Xing Liu,[1] Xiang-Ming Wang,[2] Qing-Lin Wu,[3] Hai-Peng Yu,[1] Jian Li[1]

[1]*Key Laboratory of Bio-Based Material Science and Technology (Ministry of Education), Northeast Forestry University, Harbin 150040, People's Republic of China*
[2]*Forintek Division, FP Innovations, Quebec City, Quebec, Canada G1P 4R4*
[3]*School of Renewable Natural Resources Agcenter, Louisiana State University, Baton Rouge, Louisiana 70803-6302*

Received 8 August 2009; accepted 21 May 2010
DOI 10.1002/app.32837
Published online 24 September 2010 in Wiley Online Library (wileyonlinelibrary.com).

ABSTRACT: Wood–polymer composites (WPCs) were prepared from poplar wood (*P. ussuriensis* Komarov) in a two-step procedure. Maleic anhydride (MAN) was first dissolved in acetone and impregnated into wood; this was followed by a heat process; and then, glycidyl methacrylate (GMA) and styrene (St) were further impregnated into the MAN-treated wood, followed by a second thermal treatment. Finally, the novel WPC was fabricated. The reactions occurring in the WPC, the aggregation of the resulting polymers, and their interaction with the wood substrate were analyzed by scanning electron microscopy, Fourier transform infrared spectroscopy, X-ray diffraction, and dynamic mechanical analysis. The performance of WPC was also evaluated in terms of the mechanical properties and durability, which were then correlated with the structural analysis of the WPC. The test results show that MAN and GMA/St chemically reacted with the wood cell walls in sequence, and the quantity of hydroxyl groups in the wood cell walls was evidently reduced. Meanwhile, St copolymerized with GMA or MAN, and the resulting polymers mainly filled in the wood cell lumen in an amorphous form, tightly contacting the wood cell walls without noticeable gaps. As a result, the mechanical properties, decay resistance, and dimensional stability of the WPC were remarkably improved over those of the untreated wood, and its glass-transition temperature also increased. J Appl Polym Sci 119: 3207–3216, 2011

Key words: composites; mechanical properties; modification; monomers; renewable resources

INTRODUCTION

Wood, as a natural material of biological origin, has been an essential and important raw material for human survival since their primitive state because of its high strength-to-weight ratio, unique porous structure, wide abundance, renewability, environmentally benign nature, relative ease of working, and good visual effect. Thus, wood is popular and widely used in the fields of furniture, traffic, and construction. However, despite its useful properties, wood also possesses some disadvantages, such as a variation in properties, a liability to distort with the absorption of moisture, a vulnerability to degradation by microorganisms, and a susceptibility to damage by fire; these properties greatly reduce its service life. Moreover, with the development of society, the consumption of wood has been increasing year by year, whereas the yield of high-quality wood as a structural material has been sharply decreasing. This prominent contradiction has driven researchers to look for alternative, low-quality resources for value-added applications. To achieve this goal, suitable technologies are needed to improve specific wood quality attributes (e.g., mechanical properties, dimensional stability, decay resistance, and thermal stability) to meet end-use requirements.

One of the techniques used to improve the mechanical properties and durability of low-quality solid wood that has received considerable attention in the past few decades is the formation of wood–polymer composites (WPCs). Such composites are often fabricated by the impregnation of vinyl monomers or polymeric resins with low molecular weights into void capillaries, followed by *in situ* polymerization through a catalyst–thermal treatment.[1–4] Many types of vinyl monomers and polymeric resins with low molecular weights have been explored to prepare WPCs with improved properties. These monomers include methyl methacrylate,[5] vinyl acetate,[6] styrene (St),[5] methacrylates and acrylates,[7–9] acrylonitrile,[10] and acrylamide.[11] Polymeric resins with low molecular weights include urea–formaldehyde, phenol–formaldehyde, melamine–formaldehyde

Correspondence to: Y.-X. Liu (yxliuyf@yahoo.cn) or J. Li (lyf288@yahoo.com.cn).

Contract grant sponsor: Programme of Introducing Talents of Discipline to Universities (111 Programme).

Contract grant sponsor: Key Program of the National Natural Science Foundation of China; contract grant number: 30630052.

resins,[12] and some unsaturated polyester resins.[13] However, because wood substrates contain few functional groups that are readily capable of reaction, most vinyl monomers polymerized in wood cell lumina do not fully graft with wood; this typically leads to a poor durability in WPCs.[4,14–18] Furthermore, many formaldehyde-based resins can release volatile formaldehyde from the composites and cause environmental damage.[19,20] All of these concerns have a great impact on the application and popularity of WPCs. Although some studies have been done to address these problems, on the basis of the utilization of various coupling agents and formaldehyde scavengers,[21–26] the problems have not been completely resolved, and further efforts are still needed in this field.

Coupling agents are substances that are used in small quantities to treat a surface so that bonding occurs between it and other surfaces, for example, wood and polymers.[27] They play such a very important role in improving the affinity, compatibility, and adhesion between wood cell walls and polymers in wood cell lumina that the use of a coupling agent has still been one of the most successful methods, by far, for solving these problems. The most successful coupling agents are isocyanates, anhydrides, silanes, epoxides, β-propiolactone, and methacrylates. Among these agents, maleic anhydride (MAN) and glycidyl methacrylate (GMA) are two of these most popular coupling agents; they have been widely used in traditional wood–plastic composites to bridge wood and plastics.[27] MAN is an α-, β-unsaturated carboxyl compound, containing one carbon–carbon double bonds (C=C) and two carboxylate groups (—COO—). This conjugated structure, which possesses a high activity, greatly increases MAN's reactivity with both wood and the polymer matrix; this results in crosslinking or strong adhesion at the interface. Similar to MAN, acrylic acids and methacrylates, such as methacrylic acid, epoxypropyl methacrylate, and GMA, also contain the α, β-unsaturated carbonyl structure, which may lead to crosslinking or strong interfacial adhesion.[27]

Theoretically, MAN has an active anhydride group that can react with the hydroxyl group on wood cell walls through a nucleophilic substitution reaction to create a new carboxyl-group grafting on wood cell walls (Fig. 1). The newly formed carboxyl group is not only capable of serving as a nucleophilic reagent but also capable of acting as a catalyst to provide a certain level of acidity to promote the nucleophilic substitution reaction for GMA with the carboxyl group or even the hydroxyl groups on the wood cell walls. Also, in theory, GMA can also react with the hydroxyl groups in the modified wood by its epoxy group and with St as a free-radical copolymerization through its double bond, which may produce a solid and unleachable polymer.[28,30] Moreover, some authors have reported that the occurrence of a reaction of bifunctional reagents with hydroxyl groups on wood cell walls and the copolymerization of polymeric monomers may render a crosslink between polymers in the wood cell lumen that can further create three-dimensional network structure of solid polymers grafting on wood cell walls.[28–30] Thus, WPCs with high mechanical properties and good durability can be made through a high-crosslinked polymer and its compounding with wood cell walls.

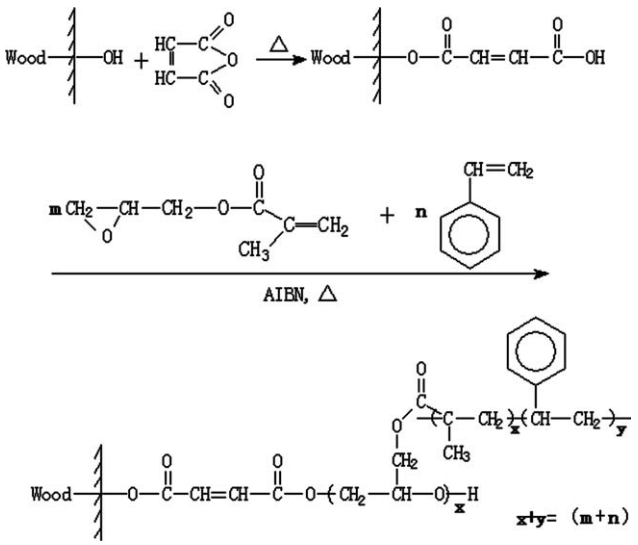

Figure 1 Schematic of the chemical reactions.

In this study, the coupling agents MAN and GMA were combined with a vinyl monomer in a two-step procedure to prepare WPCs. MAN, after being dissolved in an acetone solution, was first used to react with the hydroxyl group on the wood cell walls under a certain temperature.[21,22] GMA and St followed by *in situ* copolymerization through their double bonds, and the resulting polymers simultaneously reacted with wood modified by MAN after they were impregnated into the wood cell lumina. The objective of this study was to investigate the morphology, reaction mechanisms, mechanical properties, and durability of the resultant WPCs.

EXPERIMENTAL

Raw materials and analytical techniques

Analytical-grade GMA, purchased from Nanjing Jiulong Chemical Industry Co., Ltd. (Nanjing, China), was distilled for further purification before use. Analytical-grade St was also obtained from Nanjing Jiulong Chemical Industry; it was cleaned with sodium hydroxide, dried with anhydrous $CaCl_2$, and then distilled under vacuum pressure for further purification before use. Pyrimidine, purchased from Hubei Xinjing New Material Co., Ltd., was directly used

without any further treatment. MAN and 2,2-azobisisobutyronitrile (AIBN) were received from Shanghai Chemical Reagent Factory (Shanghai, China), and both chemicals were recrystallized before use. The wood samples of poplar lumber (Populus *ussuriensis* Komarov) selected for this study were obtained from original plantation areas in Maoershan, located in northeast China. Boards 25 × 300 × 2000 mm^3 (Radial × Tangential × Longitudinal) were machined from poplar lumber and were dried at room temperature. Test samples were then cut from these boards. The prepared samples were oven-dried at 105°C to a constant weight, and they were stored for testing.

The equipment used for the impregnation treatment was available at Northeast Forestry University. Environmental scanning electron microscopy (ESEM) tests were done with a QUANTA 200 machine (FEI Company, Hillsboro, Oregon). Fourier transform infrared (FTIR) analysis was made with a Magna IR560 spectrometer (Nicolet, Inc., Madison, WI). X-ray diffraction (XRD) tests were made with a D/max2200 instrument (Rigaku Corp., Tokyo, Japan). The test parameters selected for XRD included a Cu butt, 40 kV of voltage, 30 mA of current, a 4°/min rotating speed, and a 0.02° step distance. Dynamic mechanical analysis (DMA) was made with a DMA 242 analyzer (Netzsch, Selb, Germany), and the test parameters for three-point bending test included 60 μm of amplitude, 0.6 N of dynamic force, a 10°C/min heating rate, and 5 Hz of frequency.

Preparation of the MAN/poplar wood composites

MAN, with a few drops of pyrimidine as a catalyst, was first dissolved in acetone to prepare a mixed solution of 10% concentration. Poplar wood samples with different sizes were then immersed in the mixed solution under a vacuum of approximate 0.08 MPa for 20 min; they were then subjected to a pressure of approximate 0.8 MPa for 20 min, which was determined on the basis of previous studies.[31,32] After the pressure was released and returned to the normal atmospheric pressure, the impregnated samples were wrapped in aluminum foil and dried in an oven at 120°C for 4 h. The drying condition was found to be appropriate for the complete reaction of the impregnated samples because there was almost no obvious exothermic and/or endothermic peak in the temperature range 25–160°C. After they were unwrapped, the poplar wood samples were further vacuumed under a pressure of 0.01 MPa at room temperature to remove the residual acetone until a constant weight was reached. After this vacuum returned to normal atmospheric pressure and room temperature, MAN/poplar wood was finally obtained with a weight gain of about 8.5 ± 0.7% compared to the untreated poplar wood; this was then stored in a vacuum desiccator containing phosphorus pentoxide for further use.

Preparation of the wood/*in situ* synthetic polymer composites

AIBN, as an initiator, was first dissolved in St and GMA/St (at a 1 : 5 molar ratio) solutions, respectively, which gave a 0.5 wt % concentration of AIBN in each solution. Then, the two mixed solutions, respectively, were impregnated into the untreated poplar wood and MAN/poplar wood, which was previously extracted by acetone for 24 h under a vacuum of 0.08 MPa for 20 min and then subject to a pressure of 0.8 MPa for 20 min. After that, two types of treated wood samples of poplar wood and MAN/poplar wood were wrapped in aluminum foil and separately dried in an oven at 80 and 110°C, respectively, for 8–10 h. At last, the treated wood samples were vacuumed under 0.01 MPa and room temperature to obtain constant weights. Finally, the wood/*in situ* synthetic polymer composites with different sizes for performance evaluation, that is, polystyrene (PSt)/poplar wood and P[MAN–(GMA-*co*-St)]/poplar wood, were obtained and then stored in a vacuum desiccator containing phosphorus pentoxide for further use. The weight gain of PSt/poplar wood and P[MAN–(GMA-*co*-St)]/poplar wood was 47 ± 5.4 and 56 ± 1.9%, respectively. The conversion rate (C_r) values for the two composites were 43 ± 3.6 and 83 ± 2.7%, respectively.

The weight gain rate (W_r) and C_r were calculated with eqs. (1) and (2), respectively:

$$C_r = \frac{w_p - w_d}{w_i - w_d} \times 100\% \quad (1)$$

$$W_r = \frac{w_p - w_d}{w_d} \times 100\% \quad (2)$$

where w_p is the weight of the wood after the final treatment, w_d is the weight of the dry wood before any treatment, and w_i is the wet weight of the wood after impregnation.

Microstructure characterization and analysis of the composites

The samples for scanning electron microscopy (SEM) analysis were obtained from both PSt/poplar wood and P[MAN–(GMA-*co*-St)]/wood without acetone extraction. The interior portions of the radial and tangential planes were exposed by cutting with a surgical blade, carbon-coated, gold-sputter-coated, and then examined with the QUANTA 200 ESEM instrument at different magnifications. To obtain samples for FTIR (Magna IR560, Nicolet) and XRD

(D/max2200, Rigaku) analysis, each type of WPC sample and untreated poplar wood sample was separately ground into powder by a disintegrator and passed through a 100-mesh screen; this was followed by extraction with acetone for 24 h and toluene for 24 h and then subsequent drying to a constant weight. The samples for DMA (DMA242, Netzsch) analysis were measured with dimensions of 4 × 4 × 50 mm^3 (Radial × Tangential × Longitudinal).

Performance evaluation

The samples for the physical and mechanical tests were prepared according to the China National Standard Testing Methods for Wood Physical and Mechanical Properties (GB1928-1929-91). End-matched samples with dimensions of 20 × 20 × 300 mm^3 for the modulus of rupture test, 20 × 20 × 30 mm^3 for the compression strength test, and 20 × 20 × 50 mm^3 (Radial × Tangential × Longitudinal) for the hardness test were prepared from a pair of control and treated samples. Five specimens were used for each test. All of the mechanical property tests were performed on untreated and treated poplar wood samples with a universal testing machine (AG-10TA, Shimadzu Corp., Kyoto, Japan). During the hardness test, the indenter (a steel ball with a diameter of 11.3 mm), attached to the loading platen of the test machine, was lowered to the surface of the test specimen. A preload of 1–2 N was applied to stabilize the test specimen. The applied load was then increased to reach a target load of 1000 N in 15 s and was maintained at this force for 25 s. The actual contact area under indentation was used to calculate the hardness of the specimen. The load–deformation data were collected at a sampling rate of 10 data points per second.

Wearability testing was conducted according to the standard GB 1720-79(89). During the test, the surface of the wood samples was abraded for 5,000 revolutions by a grinding wheel on an abrasimeter. The abrasion quantities of the untreated and treated samples were calculated in terms of their reduced mass.

The impact toughness was tested on a Hatt–Turner hammering machine (Jinan Chengjin Testing Machine Co., Ltd., Jinan, China) with a drop hammer weighing 22.5 kg. The initial angle of the drop hammer and vertical position was about 60°. The results were read through the screen of the machine. End-matched samples with dimensions of 20 × 20 × 300 mm^3 (Radial × Tangential × Longitudinal) for impact toughness testing were collected to obtain a pair of control and treated samples. A minimum of 15 specimens were used for the test.

The samples, which were 20 × 20 × 20 mm^3 (Radial × Tangential × Longitudinal), for dimensional stability were evaluated by measurement of the mean volume swelling efficiency (V_m) of the 15 specimens after immersion in water for 720 h at room temperature and under atmospheric pressure according to eq. (3):

$$V_m = \frac{V_1 - V_0}{V_0} \times 100\% \quad (3)$$

where V_1 is the sample volume after immersion in water for 720 h and V_0 is the sample volume before immersion.

The decay resistance test was carried out according to the Chinese Forest Industry Standard Laboratory Methods for the Toxicity Test of Wood Preservatives to Decay Fungi. The fungus selected in this study was a brown decay fungus, named Gloeophyllum trabeum (Pers. ex Fr.) Murr. The test samples, with dimensions of 20 × 20 × 20 mm^3 (Radial × Tangential × Longitudinal), were collected to obtain a pair of control and treated samples. A minimum of five specimens were used for the test. An incubator was filled with water to a depth of 50 mm. Test samples, after being autoclaved for 30 min, were randomly placed on two mesh racks in the incubator. The relative humidity inside the incubator was 83%, and the temperature was 28°C. The samples in the incubator were evaluated according to mass loss after exposure to fungus decay for 12 weeks.

RESULTS AND DISCUSSION

Microstructure of WPC characterized with SEM

SEM micrographs of PSt/poplar wood and P[MAN–(GMA-*co*-St)]/wood are shown in Figure 2. Figure 2(a,b) clearly shows that the polymer in PSt/poplar wood filled up the wood cell lumina well in a solid form. However, the polymers did not seem to intimately contact the wood cell walls, as evidenced by obvious interface gaps between the solid polymer and the wood cell walls. Also, the polymer itself presented some clear cracks. From these observations, we deduced that St, as a single vinyl monomer, did not chemically react with the wood cell walls during polymerization; this implied poor interaction between the polymer and wood and brittleness in the polymer itself.

In contrast, as clearly shown in Figure 2(c,d), the polymers not only filled up the wood cell lumina but also intimately contacted the wood cell walls with no obvious lacunae in P[MAN–(GMA-*co*-St)]/wood, in which the wood was treated by both MAN and GMA/St. In addition, some microscratches or marks left by a knife cut during specimen preparation were also present in the polymers. From these observations, we concluded that there were strong interactions between the polymers and wood cell

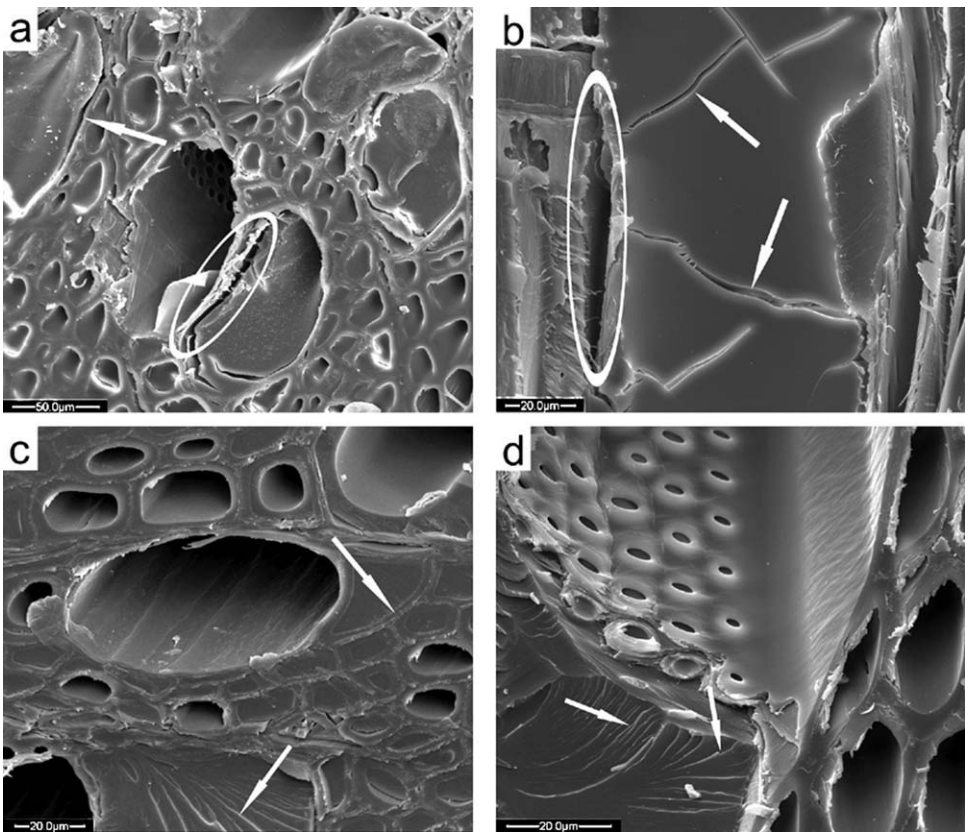

Figure 2 SEM micrographs of two poplar WPC samples: (a) PSt/poplar wood cross section (2000×), (b) PSt/poplar wood longitudinal section (2000×), (c) P[MAN–(GMA-*co*-St)]/wood cross section (1000×), and (d) P[MAN–(GMA-*co*-St)]/wood cross section (1500×).

walls, and the interactions were probably physical or chemical or a combination of both. The strong interactions could have resulted in a good complex effect of wood and polymers in the P[MAN–(GMA-*co*-St)]/wood. Moreover, the microscratches revealed on the polymers in Figure 2(c,d), left by a knife cut, may have been due to the high hardness[33] and some brittleness[34] of the polymers, which were further confirmed by the mechanical properties of P[MAN–(GMA-*co*-St)]/wood.

Analysis of the reaction with FTIR

The results of FTIR analysis of the four wood and WPC samples are given in Table I and are illustrated in Figure 3. These four samples, in order of decreasing band intensity at 1733 cm^{-1} for carbonyl stretching vibrations, were P[MAN–(GMA-*co*-St)]/wood with the highest peak, MAN/poplar wood with a high peak, PSt/poplar wood with a smaller peak, and poplar wood. This observation indicated that quite a number of carbonyl groups from MAN molecules grafted onto the wood cell walls of MAN/poplar wood, from both MAN and GMA on the wood cell walls of P[MAN–(GMA-*co*-St)]/wood as well. In other words, the carbonyl groups showing the highest intensity from both MAN and GMA grafted onto the wood cell walls of P[MAN–(GMA-*co*-St)]/wood implied that MAN was first bonded to the wood cell walls, and GMA was subsequently grafted onto the

TABLE I
Comparison of the Characteristic Groups of Two Kinds of WPCs and Their Corresponding Absorption Frequencies

Main characteristic group	Wave number (cm^{-1})	
	PSt/poplar wood	P[MAN–(GMA-*co*-St)]/wood
O—H stretching vibration (v_{O-H})	3389[37,38]	3346[37,38]
Ar—H stretching vibration ($v_{=C-H}$)	3022[38,39]	3029[37,38]
—CH_2— asymmetrical stretching vibration (v_{asC-H})	2906[35–38]	2938, 2900[35–38]
—(C=O)— stretching vibration	–	1733[35–38]
Phenyl skeletal vibration	1595[37,39]	1597, 1456[37,39]
C—O—C asymmetrical stretching vibration	–	1164[36–38]
Single and substitution Ar—H out-of-plane bending wagging (δ_{Ar-H})	704[38,39]	763, 706[38,39]

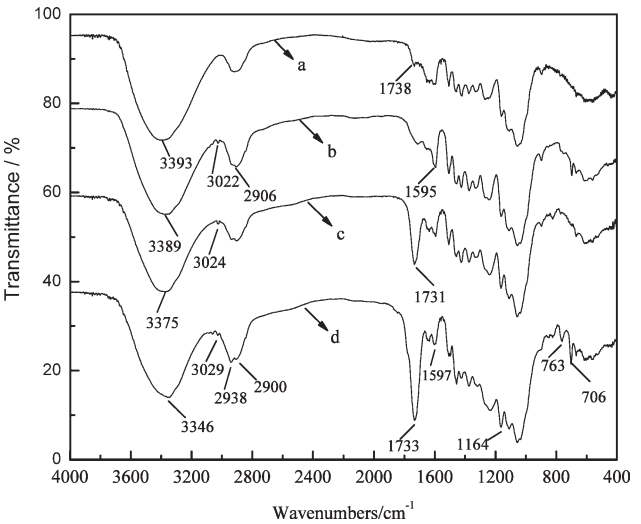

Figure 3 FTIR spectra of the four types of wood composites: (a) poplar wood, (b) PSt/poplar wood, (c) MAN/poplar wood, and (d) P[MAN–(GMA-*co*-St)]/wood.

wood cell walls by its epoxy group with a ring-opening reaction.

The peak at 3346 cm^{-1} was assigned to the stretching vibrations of hydroxyl groups for P[MAN–(GMA-*co*-St)]/wood. This peak became prominently weaker than that of PSt/poplar wood and slightly weaker than that of MAN/poplar wood and also shifted toward lower wave numbers as the intensity decreased. All of these observations suggested that the relative numbers of hydroxyl groups in wood decreased and the form of hydroxyl groups in P[MAN–(GMA-*co*-St)]/wood possibly changed to some degree after the reaction of hydroxyl groups on the wood cell walls with MAN and GMA in sequence. According to the reaction principle shown in Figure 1, we could reasonably assume that the decrease in hydroxyl groups was likely due to the nucleophilic substitution reaction of a large number of hydroxyl groups on the wood cell walls with MAN and GMA in sequence. The grafting of the polymers on the wood cell walls resulted in the decrease of the hydroxyl numbers in the whole WPC. The corresponding peak shift to lower wave numbers was probably due to the transfer of some hydroxyl groups from the wood cell walls to the polymer chains.

Figure 3 shows a slightly enhanced peak for aromatic skeletal vibrations observed at 1597 cm^{-1}, a small peak for Ar—H stretching vibrations ($\upsilon_{=C-H}$) at 3029 cm^{-1}, and two increased peaks for single and substituted Ar—H out-of-plane bending wagging (δ_{Ar-H}) at 763 and 706 cm^{-1}. All of these observations of the FTIR spectra for P[MAN–(GMA-*co*-St)]/wood suggested that the polymers grafting on the wood cell walls contained some phenyl groups, which resulted from the copolymerization of St with the other two monomers by their double bonds. However, the content of phenyl groups in the polymers seemed to be quite low. A slightly enhanced peak at 1164 cm^{-1} for C—O—C asymmetrical stretching vibrations may have been evidence for the reaction of wood hydroxyl groups with MAN and GMA in sequence, which resulted in polyethers.[40]

On the basis of the previous analyses, we concluded that under the experimental conditions that we used, MAN and GMA in sequence reacted with the hydroxyl groups of the wood cell walls, which greatly reduced the number of hydroxyl groups. Meanwhile, GMA polymerized by itself and also copolymerized with St to a certain degree. The resulting polymers were finally bonded to the wood cell walls through the polyethers resulting from the reaction of GMA with the wood hydroxyl groups and the carboxyl groups from MAN grafted on the wood cell walls as well; thus, the polymers and the wood cell walls achieved a sufficient chemical complex.

XRD analysis

The XRD curves of the unmodified poplar wood and two types of modified poplar wood are shown in Figure 4. As shown in the XRD pattern, the maximum peak values of the poplar wood, MAN/poplar wood, and P[MAN–(GMA-*co*-St)]/wood for the 002 side at $2\theta = 22.5^\circ$ were degressive in sequence, whereas the minimum wave trough values of them for the 101 side at $2\theta = 18.5^\circ$ increased in sequence. Moreover, the relative crystallinity values of the three kinds of wood samples calculated according to the Segal method [eq. (4)] decreased in sequence as well. In general, the 2θ diffraction patterns were similar for all samples, although

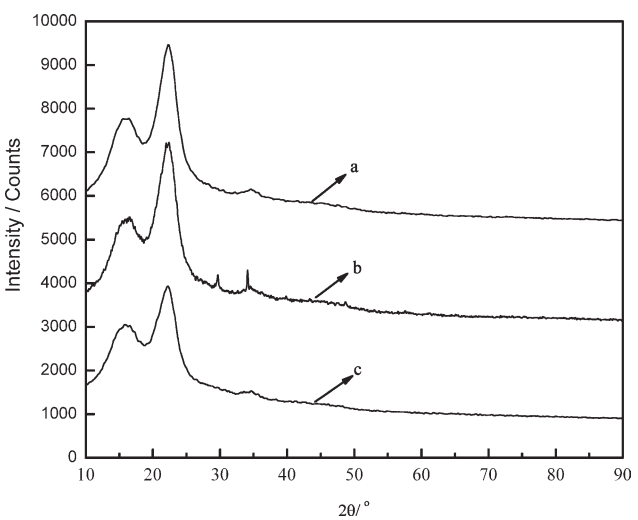

Figure 4 XRD patterns of unmodified and modified poplar wood: (a) poplar wood, (b) MAN/poplar wood, and (c) P[MAN–(GMA-*co*-St)]/wood.

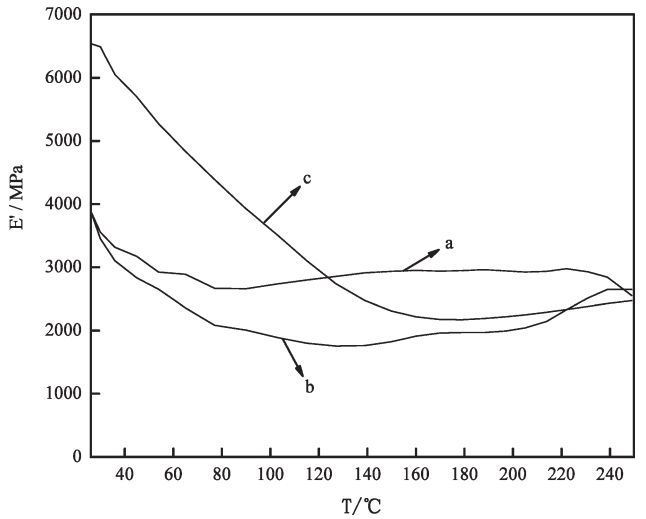

Figure 5 E′ values of treated and untreated poplar wood materials as a function of temperature (T): (a) poplar wood, (b) MAN/poplar wood, and (c) P[MAN–(GMA-*co*-St)]/wood.

there was some difference in the intensity among the samples, which represented the difference in the relative crystallinity. Compared to poplar wood, the relative crystallinity of the two treated poplar wood samples decreased; this indicated that the resulting polymers grafted onto the wood cell walls mainly remained as an amorphous form. This enhanced the proportion of amorphous components for the treated wood samples. However, the difference in the relative crystallinity for the two WPCs were probably due to either the difference in the content of the grafting amorphous components or the structural difference in their aggregation morphologies:

$$C_rI = \frac{I_{002} - I_{am}}{I_{002}} \times 100\% \quad (4)$$

where C_rI is the percentage of the relative crystallinity degree, I_{002} is the maximum intensity of the diffraction angle for the 002 side at approximately $2\theta = 22^\circ$, and I_{am} is the dispersion intensity of the noncrystalline background for the 101 side at approximately $2\theta = 18^\circ$.

Among the three wood and modified wood samples, the relative crystallinity of P[MAN–(GMA-*co*-St)]/wood was only 19.64%, which was much lower than that of MAN/poplar wood. This suggested that more amorphous polymers in P[MAN–(GMA-*co*-St)] grafted onto the wood cell walls, and thus, the polymers mainly bonded to the wood cell walls. This result was consistent with those from SEM and FTIR analyses for the WPCs.

DMA

The DMA curves of wood and modified wood materials are shown in Figure 5. In general, the storage modulus (E') of the wood and modified wood materials decreased with increasing temperature within the testing range. This was because the temperature promoted the mobility of the molecular units of each component; thus, the absorbed heat energy consumed by the resulting friction resistance caused E' to decrease. However, E' of P[MAN–(GMA-*co*-St)]/wood was the highest at the normal temperature, which demonstrated that the interaction of the produced polymers and wood cell walls was enhanced after the two-step reaction of MAN and GMA with the wood cell walls in sequence.

Figure 5 also shows that E' of MAN/poplar wood was almost the lowest in the whole temperature range and that of P[MAN–(GMA-*co*-St)]/wood sharply descended as the temperature increased. This result was probably due to the acidity of carboxyl groups produced by the grafting reaction of MAN and the wood cell walls, which degraded the wood components and resulted in more small molecules moving more freely.

Figure 6 shows the glass-transition temperatures of the treated and untreated wood materials in terms of the ratio of E' and loss modulus (E''), that is, the mechanical loss factor (tan δ), for a glass-transition temperature approximately equal to the temperature when tan δ reached maximum on the tan δ/temperature curve. The glass-transition temperature for poplar wood was 90°C, whereas higher glass-transition temperatures of 110 and 124°C were observed for P[MAN–(GMA-*co*-St)]/poplar and MAN/poplar wood, respectively. The increased glass-transition temperatures of the two WPCs indicated that the reaction of MAN and GMA/St with the wood cell walls in sequence occurred, and the interaction of

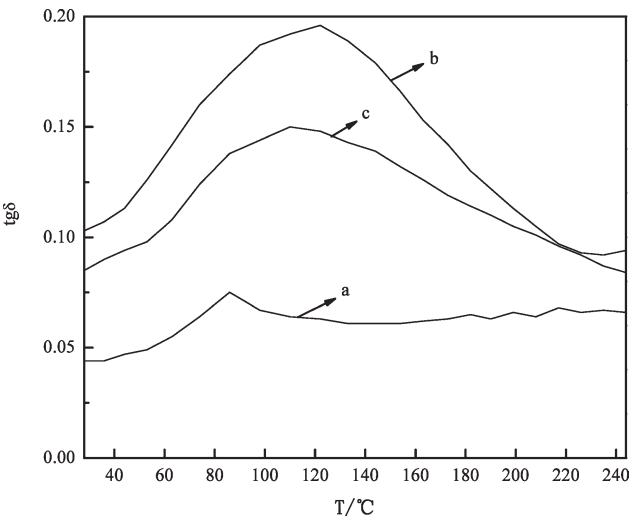

Figure 6 Tan δ values of treated and untreated poplar wood materials as a function of temperature (T): (a) poplar wood, (b) MAN/poplar wood, and (c) P[MAN–(GMA-*co*-St)]/wood.

TABLE II
Mechanical Properties of the Treated and Untreated Poplar Wood Materials

Sample	Modulus of rupture: Tangential section (MPa)	Enhanced time versus poplar wood (%)	Compressive strength: Crossing section (MPa)	Enhanced time versus poplar wood (%)
Poplar wood	57.47 (3.31)	–	51.43 (2.77)	–
PSt/poplar wood	79.59 (2.98)	38	61.98 (2.05)	21
P[MAN–(GMA-*co*-St)]/wood	86.61 (1.77)	51	118.37 (3.16)	131
Sample	Wearability: Tangential section (mm)	Enhanced time versus poplar wood (%)	Hardness: Tangential section (N)	Enhanced time versus poplar wood (%)
Poplar wood	0.101 (0.009)	–	893 (47.62)	–
PSt/poplar wood	0.041 (0.003)	59	1755 (69.14)	97
P[MAN–(GMA-*co*-St)]/wood	0.021 (0.002)	79	2260 (84.37)	153
Sample	Impact toughness: Tangential section (kJ/m^2)	Enhanced time versus poplar wood (%)		
Poplar wood	35.23 (1.66)	–		
PSt/poplar wood	15.73 (0.82)	−55		
P[MAN–(GMA-*co*-St)]/wood	23.21 (1.11)	−34		

The data in parentheses are standard deviations.

the polymers and wood cell walls was strongly enhanced; this, in turn, resulted in an improved thermal stability of the wood.

On the basis of the DMA analysis, we concluded that the interaction of the polymers and wood cell walls was highly improved after the two-step reaction of MAN and GMA/St with the wood cell walls in sequence, which increased both the glass-transition temperature and E' at normal temperature of P[MAN–(GMA-*co*-St)]/wood.

Mechanical properties

The mechanical properties of the poplar wood, PSt/poplar wood, and P[MAN–(GMA-*co*-St)]/wood are summarized in Table II. The modulus of rupture, wearability, compressive strength, and hardness were improved by 51, 79, 131, and 153%, respectively, for P[MAN–(GMA-*co*-St)]/wood and by 38, 59, 21, and 97%, respectively, for PSt/poplar wood compared to the untreated poplar wood, whereas the impact toughnesses of PSt/poplar wood and P[MAN–(GMA-*co*-St)]/wood were reduced by 55 and 34%, respectively. It was obvious that except for the impact toughness, the other mechanical properties of the poplar wood were greatly improved after the addition of MAN and GMA/St in sequence in the two-step reaction. Most of the mechanical properties of P[MAN–(GMA-*co*-St)]/wood remarkably surpassed those of the poplar wood, and all of the mechanical properties surpassed those of PSt/poplar wood.

The evidently improved mechanical properties of the treated wood were attributed to the formation of polymers with excellent performance and the good complex effect of the resulting polymers with the wood cell walls. The formation of the resulting polymers in the wood cell lumina improved the mechanical properties of the wood. The satisfactory compounding of the resulting polymers with the wood cell walls allowed the load transfer from the wood to the polymers and, thus, the part of forces passing on to the polymers, which also contributed to the improvement in the mechanical properties.

However, the impact toughnesses of both of the two treated woods decreased compared to that of the untreated poplar wood. This implied that the resulting polymers were quite brittle; this was consistent with the analysis results of SEM, and the crosslinked network may have further enhanced the brittleness. Furthermore, the microscratches observed in the SEM micrographs also confirmed the high hardness of P[MAN–(GMA-*co*-St)]/wood compared to the untreated poplar wood.

Fungal decay resistance

The test results of weight percent loss for the untreated poplar wood and three treated poplar wood samples after exposure to a brown fungus, *G. trabeum* (Pers. ex Fr.) Murr., for a period of 12 weeks are given in Table III. As illustrated by the test results, the decay resistance, in terms of weight loss for P[MAN–(GMA-*co*-St)]/wood without acetone extraction, improved by 97% compared to the untreated poplar wood, whereas it improved 54% for PSt/poplar wood compared to the untreated poplar wood and 92% for the poplar wood directly

TABLE III
Decay Resistance and Dimensional Stability of the Treated and Untreated Wood Materials

Decay resistance	Weight loss for decay resistance (%)	Enhanced time versus poplar wood (%)
Poplar wood	79.28 (3.91)	–
PSt/poplar wood	36.53 (1.63)	54
Poplar wood treated with boric compounds	6.58 (0.42)	92
P[MAN–(GMA-*co*-St)]/wood	2.28 (0.11)	97
Decay resistance	Volume swelling efficiency (%)[a]	Enhanced time versus poplar wood (%)
Poplar wood	13.21 (0.69)	–
PSt/poplar wood	11.24 (0.52)	15
P[MAN–(GMA-*co*-St)]/wood	3.93 (0.14)	70

The data in parentheses are standard deviations.
[a]The samples were soaked in water for 720 h.

treated with a water-soluble boric compound for 1% weight gain (Boric acid : Borax = 5 : 1 w/w)[41] compared to the untreated poplar wood. These results indicate that P[MAN–(GMA-*co*-St)]/wood had much better decay resistance than the untreated poplar wood and the other two treated poplar wood materials.

The improved decay resistance of P[MAN–(GMA-*co*-St)]/wood was likely attributed to the reduced water contents in the wood cell walls due to the reduction of numbers of hydroxyl groups in the wood cell walls[42,43] and the changes in the wood components due to the formation of sufficient chemical bonds between the wood cell walls and the resulting polymers,[44,45] both of which greatly destroyed the necessary environment for the existence of the brown decay fungus in wood. In addition, the chemically favorable complex of polymers and wood cell walls blocked passage of the microorganism and moisture to the wood cell walls. This also contributed to the improvement in the decay resistance for P[MAN–(GMA-*co*-St)]/wood. These test results were also supported by the FTIR analysis results: the polymers chemically bonded to the wood cell walls after the two-step reaction of MAN and GMA/St with the wood cell walls in sequence.

Dimensional stability

The results of volume swelling efficiency are also given in Table III. The volume swelling efficiency of P[MAN–(GMA-*co*-St)]/wood without acetone extraction was reduced by 70% compared to the untreated poplar wood after it was soaked in water for 720 h and by 15% for PSt/poplar wood compared to the untreated poplar wood. The improvement in the volume swelling efficiency for P[MAN–(GMA-*co*-St)]/wood was probably due to the replacement of the hydroxyl groups on the wood cell walls by the relatively hydrophobic polymers of P[MAN–(GMA-*co*-St)]; this resulted in a large reduction in hygroscopic sites (hydroxyl groups), and thus, the penetration of water into the wood cell walls was markedly reduced. Furthermore, the resulting polymers, with obvious hydrophobic characteristics, also reduced the water content in the wood cell lumina. All of these improvements resulted in a higher dimensional stability for P[MAN–(GMA-*co*-St)]/wood compared to PSt/poplar wood and the untreated poplar wood.

CONCLUSIONS

On the basis of the characterization and analysis of novel wood/*in situ* synthetic polymer composites and their performance tests, we drew the following conclusions:

The structure of P[MAN–(GMA-*co*-St)]/wood, characterized by SEM, FTIR spectroscopy, XRD, and DMA, showed that polymers mainly existed in the wood cell lumina as an amorphous form and were chemically bonded to the wood cell walls. Thus, the polymers tightly contacted the wood cell walls; this resulted in a higher glass-transition temperature for the WPCs compared with the untreated poplar wood.

Most of the mechanical and physical properties of P[MAN–(GMA-*co*-St)]/wood, including the modulus of rupture, wearability, compressive strength, and hardness, were significantly improved compared to the untreated poplar wood. The durability of the WPCs, involving the dimensional stability and decay resistance, was also evidently improved.

In general, the performance of the low-grade poplar wood was significantly improved to a large extent with the new two-step process, which appears to be a promising method for the chemical modification of wood.

The authors extend special thanks to Dr. Zhang Yaolin (Forintek Division, FP Innovations) for helpful comments.

References

1. Sheikh, N.; Taromi, F. A. Radiat Phys Chem 1993, 42, 179.
2. Elias, H. B.; Numan, S. Radiat Phys Chem 2003, 66, 49.
3. Marc, H. S.; Svetlana, V.; Stig, L.; Jonathan, G. P. Wood Sci Technol 2003, 37, 165.
4. Ümit, C. Y.; Sibel, Y.; Enqin, D. G. Bioresour Technol 2005, 96, 1003.
5. Michel, F. C.; Kenneth, G.; Marc, H. S. Wood Sci Technol 1996, 30, 179.
6. Ellis, D. W. Wood Fiber Sci 1994, 26, 333.
7. Mathias, L. J.; Lee, S.; Wright, J. R.; Warren, S. C. J Appl Polym Sci 1991, 42, 55.

8. Rozman, H. D.; Kumar, R. N.; Abusamah, A.; Saad, M. J. J Appl Polym Sci 1998, 67, 1221.
9. Ellis, D. W.; O'Dell, J. L. J Appl Polym Sci 1999, 73, 2493.
10. Dilek, S.; Olgun, G. Radiat Phys Chem 1995, 46, 889.
11. Elias, H. B.; Numan, S.; Ibrahim, O. Radiat Phys Chem 2002, 64, 277.
12. Gindl, W.; Zargar, Y. F.; Wimmer, R. Bioresour Technol 2003, 87, 325.
13. Zaki, A. Radiat Phys Chem 2006, 75, 1075.
14. Mozafer, H. M.; Mubaralc, A. K.; Azam, A. M.; Idriss, A. K. M.; Mustafa, I. Radiat Phys Chem 1996, 48, 781.
15. Dilek, S.; Olgun, G. Radiat Phys Chem 1999, 54, 583.
16. Tmimar, M. C.; Pitman, A.; Mihai, M. D. Int Biodeterior Biodegrad 1999, 43, 181.
17. Evans, P. D.; Wallis, A. F. A.; Owen, N. L. Wood Sci Technol 2000, 34, 151.
18. Kartal, S. N.; Yoshimura, T.; Imamura, Y. Int Biodeterior Biodegrad 2004, 53, 111.
19. Furuno, T.; Imamura, Y.; Kajita, H. Wood Sci Technol 2004, 37, 349.
20. Shi, J. S.; Li, J. Z.; Zhou, W. R.; Zhang, D. R. J Beijing Forestry Univ 2006, 28, 123 (In Chinese).
21. Minoru, U.; Hideaki, M.; Yutaka, M. Mokuzai Gakkaishi 1992, 38, 458.
22. Minoru, U.; Hideaki, M.; Yutaka, M. Mokuzai Gakkaishi 1994, 40, 725.
23. Rashmi, R. D.; Ilias, A.; Maji, T. K. Bioresour Technol 2003, 88, 185.
24. Souloungangа, P.; Loubinoux, B.; Wozniak, E.; Lemor, A.; Gérardin, P. Holz Roh Werkst 2004, 62, 281.
25. Elvy, S. B.; Dennis, G. R.; Ng, L. T. J Mater Process tech 1995, 48, 365.
26. Christian, H.; Günther, W.; Wolfgang, G. Wood Sci Technol 2005, 39, 502.
27. Lu, J. Z.; Wu, Q. L., Jr.; Mcnabb, H. S. Wood Fiber Sci 2000, 32, 88.
28. Rozman, H. D.; Banks, W. B.; Lawther, M. L. J Polym Mater 1994, 26, 19.
29. Yoshiharu, M.; Yoshiyuki, N.; Noritaka, K.; Hidematsu, S.; Minoru, I. Polymer 1996, 37, 1949.
30. Rozman, H. D.; Kumar, R. N.; Abdul Khalil, H. P. S.; Abusamah, A.; Abu, R.; Ismail, H. Eur Polym J 1997, 33, 1213.
31. Zhang, Y. L.; Wan, H.; Zhang, S. Y. Holzforschung 2005, 59, 322.
32. Zhang, Y. L.; Zhang, S. Y.; Yang, D. Q.; Wan, H. J Appl Polym Sci 2006, 102, 5085.
33. Dasaria, A.; Yu, Z. Z.; Mai, Y. W. Mater Sci Eng R 2009, 63, 31.
34. Han, J.; Robert, B.; Sue, H. J. Polymer 2009, 50, 4056.
35. Zou, P.; Xiong, H. G.; Tang, S. W. Carbohydr Polym 2008, 73, 378.
36. Sailaja, R. R. N. Compos Sci Technol 2006, 66, 2039.
37. Bodîrlău, R.; Teacă, C. A.; Spiridon, I. Bioresources 2009, 4, 1285.
38. Martínez-Pardo, M. E.; Cardoso, J.; Vázquez, H.; Aguilar, M. Nucl Instrum Methods Phys Res B 1998, 140, 325.
39. Rutkowski, P. Waste Manage 2009, 29, 2983.
40. Zhou, Y. Z.; Tan, X. M.; Yu, G. F.; Xie, H. Q. Polym Mater Sci Eng 2000, 16, 69.
41. Baysal, E.; Yalinkilic, M. K.; Altinok, M.; Sonmez, A.; Peker, H.; Colak, M. Constr Build Mater 2007, 21, 1879.
42. Chang, H. T.; Chang, S. T. Bioresour Technol 2002, 85, 201.
43. Eiichi, O.; Sakae, S.; Kazuya, M. J Wood Sci 2007, 53, 408.
44. Kazuya, M.; Ryosulce, T.; Kenji, O. J Wood Sci 2003, 49, 519.
45. Wang, Y.; Kazuya, M.; Ikuho, I. J Wood Sci 2007, 53, 94.